

## DRAFT: WTC2005-63382

### ADHESION IN THE CONTACT OF A SPHERICAL INDENTER WITH A LAYERED MEDIUM

Asri Onur Sergici, George G. Adams, Sinan Müftü  
Department of Mechanical and Industrial Engineering  
Northeastern University  
Boston, MA 02115, USA

#### ABSTRACT

With the emergence of micro- and nano-technology, the contact mechanics of MEMS & NEMS devices and components is becoming more important. The motivation for this work is to gain a better understanding of the role of coatings and thin films on micro- and nano-scale contact phenomena, and to understand the interactions of measurement devices, such as an Atomic Force Microscope (AFM), with layered media.

The frictionless contact between a rigid spherical indenter and an elastic layered medium is the subject of this research. This configuration can be viewed as either a single asperity contact or as a building block of a multi-asperity rough surface contact model. As the scale decreases to the nano level, adhesion becomes an important issue in this contact problem. The presence of adhesion affects the relationships among the applied force, the penetration of the indenter and the size of the contact area. This axisymmetric problem includes the effect of adhesion using the Maugis model. This model spans the range of the Tabor parameter between the JKR and DMT regions. Key parameters have been identified which are the elastic moduli ratio of the layer and the substrate, the Poisson's ratios, the dimensionless contact radius, the dimensionless layer thickness, and the adhesion parameter  $\lambda$ .

#### INTRODUCTION

The axisymmetric contact problem with an elastic layer (Civelek et al., 1974) and the effect of coatings on contact (Chen et al., 1972) are well-investigated. Recently Johnson and Sridhar (2001) used a JKR type of formulation for the finite element analysis of the adhesion of a sphere on a layered elastic medium. In the present investigation, the Maugis (1992) adhesion model is applied to the contact of a spherical indenter with a layered elastic half-space. The configuration is shown in Figure 1. An elastic layer (1) of thickness  $h$  is perfectly bonded to an elastic substrate (2). It is indented by a rigid sphere of radius  $R$  with a load  $P$ . The penetration depth is denoted by  $\delta$ . Contact between the indenter and the surface is assumed to be frictionless.

#### FORMULATION

Boundary conditions at the interface are perfectly bonded and at the free surface ( $z = -h$ ) are:

$$\left. \begin{aligned} \tau_{rz}(r, -h) &= 0 & , & \quad r > 0 \\ u_z(r, -h) &= \delta - f(r) & , & \quad r < a \\ \sigma_{zz}(r, -h) &= 0 & , & \quad r > a \end{aligned} \right\} \text{Mixed B.C.}$$

where  $f(r)$  is the shape of the indenter. Harmonic Papkovitch-Neuber potentials are chosen:

$$\nabla^2 \varphi_z = 0 \quad , \quad \nabla^2 \phi = 0 \quad , \quad (\varphi_r, \varphi_\theta = 0)$$

Displacements and stresses calculated from these potentials satisfy the equations of elasticity – equilibrium, compatibility, and stress-strain laws.

The effect of the adhesion is included using Maugis model. A uniform tensile stress ( $\sigma_0$ ) is assumed to exist between the contacting asperities just outside the contact zone,  $a < r < c$ , where the surfaces separate by a distance less than  $h_0$ . The maximum stress and the work of adhesion are chosen to match those of the Lennard-Jones potential, which gives  $h_0 = 0.97 z_0$ , where  $z_0$  is the equilibrium separation. Including adhesion, the final equation becomes a singular integral equation with a Cauchy-type singularity which can be solved numerically (Erdogan et al., 1972):

$$u_z(r, -h) = - \int_0^a \varepsilon \sigma_{zz}(\varepsilon) k_1(\varepsilon, r) d\varepsilon - \int_0^a \varepsilon \sigma_{zz}(\varepsilon) k_2(\varepsilon, r) d\varepsilon \\ - \sigma_0 \int_0^c \varepsilon k_1(\varepsilon, r) d\varepsilon - \sigma_0 \int_0^c \varepsilon k_2(\varepsilon, r) d\varepsilon$$

where the kernels  $k_1(\varepsilon, r)$  and  $k_2(\varepsilon, r)$  depend on the shear moduli ratio ( $\mu_1/\mu_2$ ), and the Poisson's ratios  $\nu_1$  and  $\nu_2$ .

Using the following normalizations, the parameters in the Sergici-Adams-Müftü (SAM) model become  $A$ ,  $H$ ,  $\lambda$ , ( $\mu_1/\mu_2$ ),  $\nu_1$  and  $\nu_2$ :

$$A = \frac{a}{\left(\frac{\pi w R^2}{K}\right)^{1/3}} \quad , \quad H = \frac{h}{\left(\frac{\pi w R^2}{K}\right)^{1/3}} \quad , \quad \lambda = \frac{2 \sigma_0}{\left(\frac{\pi w K^2}{R}\right)^{1/3}}$$

$$\text{where } K = \frac{8}{3} \left( \frac{\mu_1}{1 - \nu_1} \right) \text{ and } w = \sigma_0 h_0 .$$

#### RESULTS

Results are given for the dimensionless contact radius vs. the dimensionless normal force, and the dimensionless normal force vs. the dimensionless penetration depth for a wide range of parameters. Figures 2 and 3 reflect the effect of the elastic moduli ratio, covering the range  $0.05 < (\mu_1/\mu_2) < 10$ . Figures 4 and 5 show the results for different adhesion parameters,  $0.05 < \lambda < 5$ .

**REFERENCES**

Chen, W. T., and Engel, P. A., 1972, "Impact and contact stress analysis in multilayer media," *Int. J. Solids Structures*, Vol. 8, pp. 1257-81.

Civelek, M. B., and Erdogan, F., 1974, "The axisymmetric double contact problem for a frictionless elastic layer," *Int. J. Solids Structures*, Vol. 10, pp. 639-59.

Erdogan, F., and Gupta, G. D., 1972, "On the numerical solution of singular integral equations," *Q. Appl. Math.*, Vol. 29, pp. 525-34.

Johnson, K. L., 1985, *Contact Mechanics*, 1st ed., Cambridge University Press, 456 pp.

Johnson, K. L., and Sridhar, I., 2001, "Adhesion between a spherical indenter and an elastic solid with a compliant elastic coating" *J. Phys. D: Appl. Phys.*, Vol. 34, pp. 683-9.

Maugis, D., 1992, "Adhesion of spheres: the JKR-DMT transition using a Dugdale model," *J. Coll. and Interface Sci.*, Vol. 150, pp. 243-69.

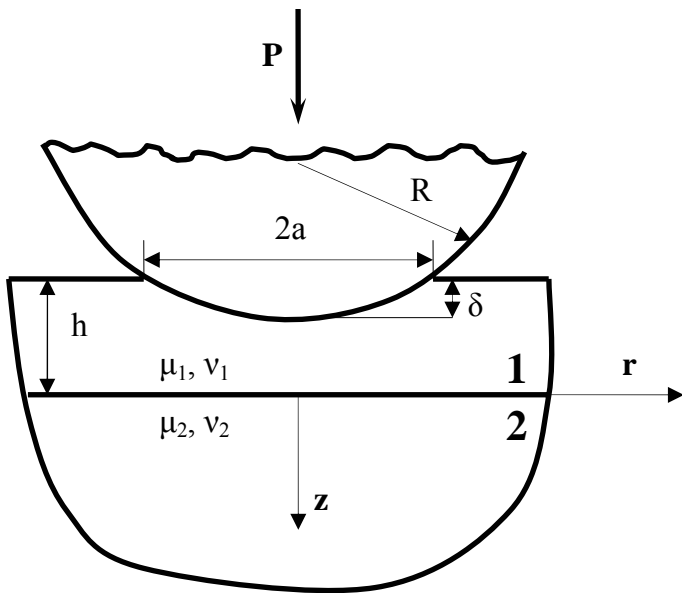


**Figure 1.** Indentation of an elastic layered media.

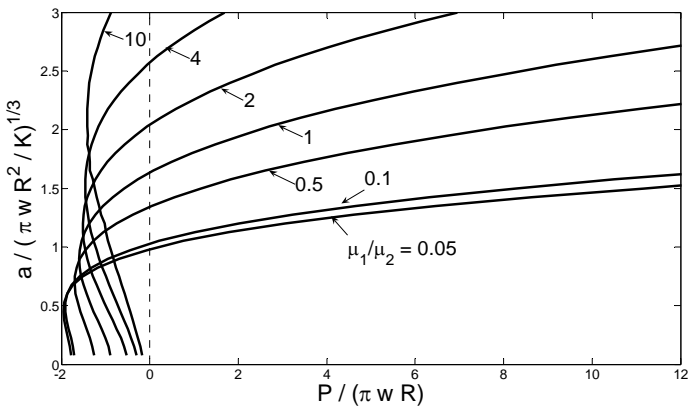


**Figure 2.** Variation of the dimensionless contact radius with the dimensionless normal force for various  $\mu_1/\mu_2$  values, with  $H = 0.2, \lambda = 1,$  and  $\nu_1 = \nu_2 = 1/3$ .

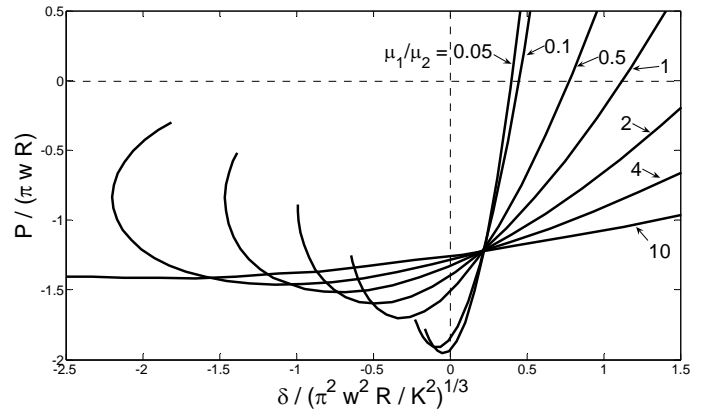


**Figure 3.** Variation of the dimensionless normal force with the dimensionless penetration depth for various  $\mu_1/\mu_2$  values, with  $H = 0.2, \lambda = 1,$  and  $\nu_1 = \nu_2 = 1/3$ .

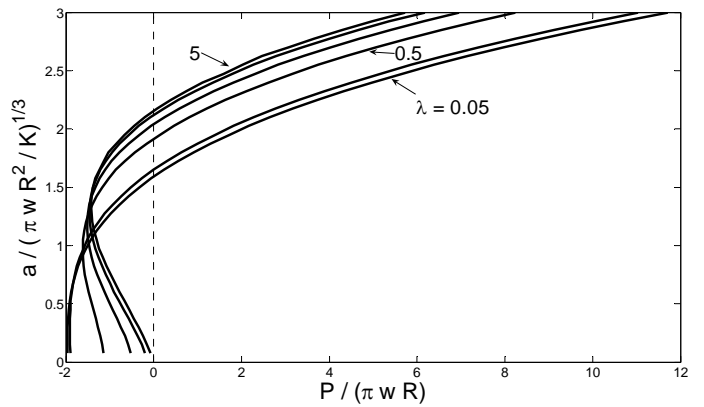


**Figure 4.** Variation of the dimensionless contact radius with the dimensionless normal force for various  $\lambda$  values, with  $H = 0.2, \mu_1/\mu_2 = 2,$  and  $\nu_1 = \nu_2 = 1/3$ .

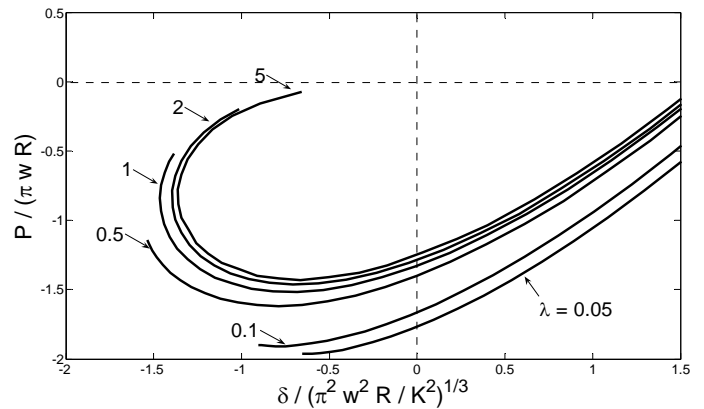


**Figure 5.** Variation of the dimensionless normal force with the dimensionless penetration depth for various  $\lambda$  values, with  $H = 0.2, \mu_1/\mu_2 = 2,$  and  $\nu_1 = \nu_2 = 1/3$ .